arXiv:1603.03744v4 [physics.acc-ph] 18 May 2016

Transverse Mode Coupling Instability with Space Charge

V. Balbekov*
Fermi National Accelerator Laboratory
P.O. Box 500, Batavia,
Illinois 60510, email balbekov@fnal.gov
(Dated: May 20, 2016)

Transverse mode coupling instability of a bunch with space charge and wake field is considered within the frameworks of the boxcar model. Eigenfunctions of the bunch without wake are used as a basis for solution of the equations with the wake field included. Dispersion equation for the bunch eigentunes is presented in the form of an infinite continued fraction and also as the recursive relation with arbitrary number of the basis functions. It is shown that the influence of space charge on the instability essentially depends on the wake sign. In particular, threshold of the negative wake increases in absolute value until the space charge tune shift is rather small, and goes down at the higher space charge. The explanation is developed by analysis of the bunch spectrum.

PACS numbers: 29.27.Bd

I. INTRODUCTION

Transverse Mode Coupling Instability has been observed first in PETRA and has been explained by Kohaupt on the base of two-particle model [1]. Many papers concerning this effect were published later, including handbooks and surveys (see e.g. [2]). It is established that the instability occurs by a coalescence of two neighboring head-tail modes due to the bunch wake field.

TMCI with space charge was considered first by Blaskiewicz [3]. The main conclusion which has been done in the paper and many times quoted is that SC enhances the TMCI threshold that is improve the beam stability.

The problem has been investigated later in the case of high space charge when the tune shift significantly exceeds synchrotron tune [4, 5]. It was confirmed that SC can stabilize TMCI suppressing the instability in considered limiting case ("vanished TMCI" [4]). However, it was shown in Ref. [5] that this statement can be true only for negative wakes whereas positive ones impair the stability resulting in a monotonous falling of the TMCI threshold when the SC tune shift increases. Besides, it was suggested in Ref. [4] that the threshold growth of negative wake can also cease and turn back if the space charge tune shift exceeds synchrotron tune on one or two orders of value.

Numerical simulations of the instability with a modest tune shift have confirmed these results on the whole demonstrating the predicted effects with positive and negative wakes [6]

So-termed three-mode model has been developed in Ref. [7] for analytical description of the TMCI with chromaticity and arbitrary wake at moderate SC. The results of this simple model are in a good agreement with those mentioned above.

However, it would be premature to declare the problem settled because there are some lacunae and contradictions in the cited papers.

A non-monotonic dependence of the TMCI threshold and rate on the SC tune shift has been actually obtained in Ref. [3]. It has been shown that the stability and instability regions can change each other when the tune shift increases. Besides, it appeared that the applied expansion technique does not always converge as more basis vectors are added.

The numerical solutions in Ref. [6] sometimes demonstrate a non-monotonic dependence of the threshold on the tune shift as well. However, the number of examples looks insufficient for any reliable conclusions about the crucial value of the shift.

The statements of papers [4] and [5] relating to the negative wakes are questionable because negative multipoles ($m < 0$) have been excluded from the consideration due to the basis assumptions. Meanwhile, it is known that the coupling of the multipoles $m = 0$ and $m = -1$ is the main factor resulting in the TMCI without space charge.

Only the case of modest space charge $\Delta Q_{sc}/Q_s < 3$ has been investigated in Ref. [7] demonstrating that the TMCI threshold of negative wake goes up when the tune shift increases. However, used equations allow to suggest that a sudden kink of the threshold curve is possible at the higher shift. Therefore, field of application of the three-mode model is still an open question. A verification and an explanation of these results are desirable.

These problems are considered in the presented paper based on the analysis of a square bunch (the boxcar model). An advantage of such a model is that set of its eigenmodes without wake is known exactly, providing very convenient basis for the consideration of the TMCI problem in depth.

II. BASIC EQUATIONS AND ASSUMPTIONS

The terms, basic symbols and equations of Ref. [5] and [7] are used in this paper. In particular, linear syn-

*Electronic address: balbekov@fnal.gov

chrotron oscillations are considered here being characterized by amplitude A and phase ϕ, or by corresponding Cartesian coordinates:

$$\theta = A\cos\phi, \qquad u = A\sin\phi.$$

Thus θ is the azimuthal deviation of a particle from the bunch center in the rest frame, and variable u is proportional to the momentum deviation about the bunch central momentum (the proportionality coefficient plays no part in the paper). Transverse coherent displacement of the particles in some point of the longitudinal phase space will be presented as real part of the function

$$X(A,\phi,t) = Y(A,\phi)\exp\left[-i(Q_0+\zeta)\,\theta - i\,(Q_0+\nu)\,\Omega_0 t\right] \tag{1}$$

where Ω_0 is the revolution frequency, Q_0 is the central betatron tune, and ν is the tune addition produced by space charge and wake field. Generally, ζ is the normalized chromaticity, however, only the case $\zeta = 0$ will be investigated in this paper. Besides, we restrict the consideration by the simplest case of the wake field which has constant value within the bunch being zero behind it. Then the function Y satisfies the equation [5],[7]:

$$\nu Y + i\,Q_s\frac{\partial Y}{\partial\phi} + \frac{\Delta Q(0)\rho(\theta)}{\rho(0)}\left[Y(\theta,u) - \bar{Y}(\theta)\right] = 2q\int_\theta^\infty \bar{Y}(\theta')\rho(\theta')d\theta' \tag{2}$$

where $F(\theta,u)$ and $\rho(\theta)$ are normalized distribution function and corresponding linear density of the bunch, Q_s is the synchrotron tune, $\Delta Q(\theta)$ is the space charge tune shift, and $\bar{Y}(\theta)$ is the bunch displacement in usual space which can be found by the formula

$$\rho(\theta)\bar{Y}(\theta) = \int_{-\infty}^{\infty} F(\theta,u)Y(\theta,u)\,du \tag{3}$$

Parameter q is the reduced wake strength which is connected with the usual wake field function W_1 by the relation:

$$q = \frac{r_0 RNW_1}{8\pi\beta\gamma Q_0} \tag{4}$$

with $r_0 = e^2/mc^2$ as the classic radius of the particle, R as the accelerator radius, N as the bunch population, β and γ as normalized velocity and energy. More often than not, this parameter is negative, at least within the bunch. The typical and very known example is the resistive wall wake [2]. However, positive wake function is possible as well. For example, it can be created by heavy positive ions arising at ionization of residual gas by proton beam. This kind of instability has been observed in CPS [9] and U-70 [10]. Therefore, constant wakes of both signs will be examined in this paper.

Solution of Eq. (2) can be found by its expansion in terms of the eigenfunctions of corresponding uniform equation which is

$$\nu_j Y_j + i\,Q_s\frac{\partial Y_j}{\partial\phi} + \frac{\Delta Q(0)\rho(\theta)}{\rho(0)}\left[Y_j(\theta,u) - \bar{Y}_j(\theta)\right] = 0 \tag{5}$$

It is easy to check that they form the orthogonal basis with the weighting function $F(\theta,u)$. Besides, we will impose the normalization condition:

$$\int\int F(\theta,u)Y_j^*(\theta,u)Y_k(\theta,u)\,d\theta du = \delta_{jk} \tag{6}$$

where the star means complex conjugation. Then, looking for the solution of Eq. (2) in the form

$$Y = \sum_j C_j Y_j, \tag{7}$$

one can get the relation for the unknown coefficients C_j:

$$\sum_j(\nu-\nu_j)C_jY_j = 2q\sum_j C_j\int_\theta^\infty \bar{Y}_j(\theta')\rho(\theta')d\theta' \tag{8}$$

where $\bar{Y}_j$ and Y_j are also connected by Eq. (3). Multiplying Eq. (8) by factor $F(\theta,u)Y_J^*(\theta,u)$, integrating over $d\theta du$, and using normalization condition (6) one can get series of equations for the coefficients C:

$$(\nu-\nu_J)C_J = 2q\sum_j C_j\int_{-\infty}^{\infty}\rho(\theta)\bar{Y}_J^*(\theta)\,d\theta\int_\theta^\infty \rho(\theta')\bar{Y}_j(\theta')\,d\theta', \tag{9}$$

III. BOXCAR MODEL

The boxcar model is characterized by following expressions for the bunch distribution function and its linear density:

$$F = \frac{1}{2\pi\sqrt{1-A^2}} = \frac{1}{2\pi\sqrt{1-\theta^2-u^2}}, \tag{10a}$$

$$\rho(\theta) = \frac{1}{2} \qquad \text{at} \qquad |\theta| < 1 \tag{10b}$$

Because the eigenfunctions depend on two variables (θ-u) (or A-ϕ), it is more convenient to represent j as a pair of the indexes:

$$j \equiv \{n,m\}, \qquad Y_j \equiv Y_{n,m}$$

Analytical solutions of Eq. (5) for the boxcar model have been obtained in such a form by Sacherer [8]. The most important point is that the averaged eigenfunctions $\bar{Y}_{n,m}$ do not depend on second index being proportional to the Legendre polynomials: $\bar{Y}_{n,m}(\theta) = \bar{Y}_n(\theta) \propto P_n(\theta)$, $n = 0, 1, 2, \ldots$. At any n,, there are $n+1$ different eigenmodes $Y_{n,m}(\theta,u)$ which satisfy the equation

$$(\nu_{n,m} + \Delta Q)\,Y_{n,m} + i\,Q_s\frac{\partial Y_{n,m}}{\partial\phi} = \Delta Q\,S_{n,m}P_n(\theta) \tag{11}$$

where $m = n, n-2, \ldots, -n$. Coefficients $S_{n,m}$ are added to the right-hand part of this equation so that the

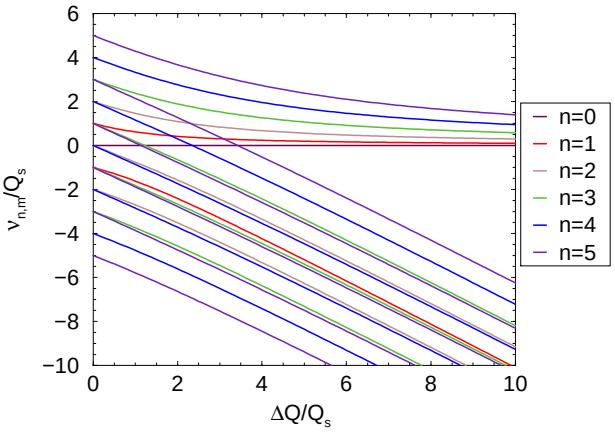

FIG. 1: Eigentunes of the boxcar bunch without wake. With any n, there are $n+1$ eigentunes starting from different points at $\Delta Q = 0$.

eigenfunctions met normalization condition (6). Details of the calculation are represented in the Appendix, and several eigentunes $\nu_{n,m}$ are plotted in Fig. 1. It is seen that all the lines take start from the points $\nu_{n,m} = mQ_s$ at $\Delta Q = 0$. It is the commonly accepted rule to use the term 'multipole' for the collective synchrotron oscillations of such frequency, so m should be treated here as the multipole number. Another index n characterizes the eigenfunction power which property is usually associated with the radial mode number when the lower number means the lower power. Because $n \geq |m|$, the mode $\{m, m\}$ should be treated as the lowest radial mode of m-th multipole. At $\Delta Q \neq 0$, the multipoles mix together and the eigentunes break down into 2 groups. In the first of them, all tunes have positive value which tends to 0 at $\Delta Q \to \infty$. It is seen that they are the lowest radial modes by the origin. In second group, the tunes are about $\nu_{n,m} \simeq mQ_s - \Delta Q$ being weakly dependent on the radial index n.

With $\bar{Y}_{n,m} = S_{n,m}P_n(\theta)$, series (9) for the boxcar bunch obtains the form

$$(\nu - \nu_{NM})C_{NM} = q\, S^*_{NM} \sum_{n=0}^{\infty} R_{Nn} \sum_m S_{nm}C_{nm} \qquad (12)$$

with the matrix

$$R_{Nn} = \frac{1}{2}\int_{-1}^{1} P_N(\theta)\, d\theta \int_{\theta}^{1} P_n(\theta')\, d\theta' \qquad (13)$$

Its small fragment is shown in Tab. I, whereas the general form at $N \neq 0$ is

$$R_{N,n} = -\frac{\delta_{N-1,n}}{(2N-1)(2N+1)} + \frac{\delta_{N+1,n}}{(2N+1)(2N+3)} \qquad (14)$$

It is convenient to use the terms

$$Z_n = \sum_m S_{n,m}C_{n,m} \qquad (15a)$$

TABLE I: Fragment of the matrix $R_{N,n}$. Its general form is given by Eq. (13) and (16).

$n \to$	0	1	2	3	4	5
$N=0$	1	1/3	0	0	0	0
$N=1$	−1/3	0	1/15	0	0	0
$N=2$	0	−1/15	0	1/35	0	0
$N=3$	0	0	−1/35	0	1/63	0

$$W_n(\nu) = \sum_m \frac{|S_{n,m}|^2}{\nu - \nu_{n,m}} \qquad (15b)$$

Then Eq. (12) can be reduced to the form

$$Z_N = q\, W_N \sum_{n=0}^{\infty} R_{N,n}Z_n \qquad (16)$$

It is easy to show that $\nu_{0,0} = 0$, $S_{0,0} = 1$, that is $W_0 = 1/\nu$. Using these features and Eq. (14) one can represent the solvability condition of series (16), that is dispersion equation for the bunch eigentunes, in terms of infinite continued fraction

$$\nu - q + \cfrac{(q/3)^2 W_1}{1 + \cfrac{(q/15)^2 W_1 W_2}{1 + \cfrac{(q/35)^2 W_2 W_3}{1 + \cdots\cdots}}} = 0 \qquad (17)$$

This expression has to be truncated in reality by applying of the assumption $W_n = 0$ at $n \geq n_{\max}$. Assigning corresponding truncated expression as $T_{n_{\max}}$, one can write the approximate dispersion equation as

$$T_{n_{\max}}(\nu) = 0 \qquad (18)$$

with following recurrent relations:

$$T_n = T_{n-1} + T_{n-2}\frac{q^2 W_{n-1}W_n}{(4n^2-1)^2}, \qquad (n \geq 2) \qquad (19)$$

and the initial conditions:

$$T_0 = \nu - q, \qquad (20a)$$

$$T_1 = \nu - q + \left(\frac{q}{3}\right)^2 \frac{3(\nu + \Delta Q)}{\nu(\nu + \Delta Q) - Q_s^2} \qquad (20b)$$

IV. THREE-MODE APPROXIMATION

Eq. (18) is trivial at $n_{\max} = 0$: $T_0 = 0$ that is $\nu = q$. It describes the wake contribution to the tune of the lowest (rigid) eigenmode of the bunch. Of course, TMCI can not appear in this approximation, and the simplest equation to disclose it is $T_1(\nu) = 0$ that is, in accordance with Eq. (19)-(20),

$$(\nu - q)\left(\nu - \frac{Q_s^2}{\nu + \Delta Q}\right) = -\frac{q^2}{3} \qquad (21)$$

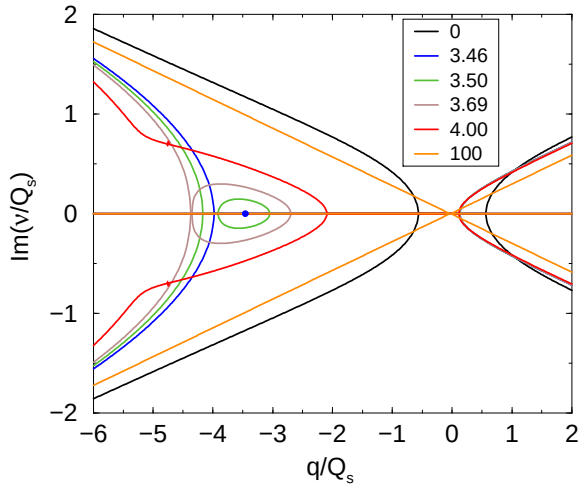

FIG. 2: Imaginary part of the boxcar eigentunes against the wake strength at different value of the space charge tune shift. Two regions of instability occur with negative wake at $3.46 < \Delta Q/Q_s < 3.69$.

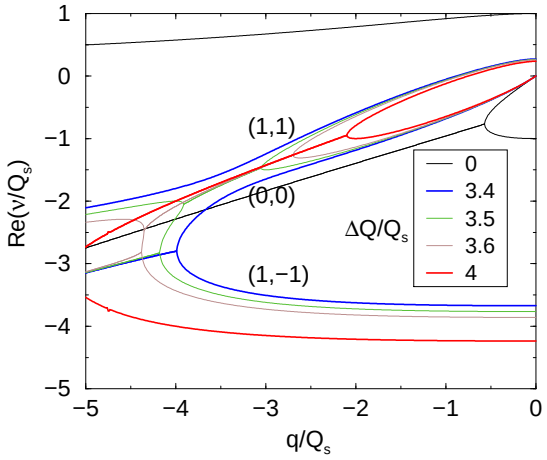

FIG. 3: Real part of the boxcar eigentunes against the wake strength at different space charge tune shift. With negative wake, coalescence of the modes $\{0,0\}+\{1,-1\}$ causes the instability at $\Delta/Q_s < 3.46$ (blue lines). The switching on the modes $\{0,0\}+\{1,1\}$ happens at $\Delta Q/Q_s > 3.69$ (red lines).

This third order equation absolutely coincides with Eq. (7.3) of Ref. [7] (without chromaticity) despite the fact that very different concepts have been used to derive them. However, the examples presented in [7] have been restricted by the modest space charge: $\Delta Q/Q_s < 3$. The situation beyond this region should be explored for further development of the techniques.

Some solutions of Eq. (21) are shown in Fig. 2 and Fig. 3. Their behavior is clear if the wake is positive: the TMCI threshold goes down monotonically when the space charge increases. The case of negative wake is more complicated and requires special comments.

The imaginary part of the solutions is plotted against q/Q_s in Fig. 2. According to the plot, the instability threshold is $|q_{\rm th}/Q_s| = 0.567$ at $\Delta Q/Q_s = 0$ (the black lines). Then it moves to the left (that is increases in absolute value) reaching $q_{\rm th}/Q_s \simeq -4$ at $\Delta Q/Q_s = 3.46$ (blue line). The picture crucially changes after that because new region of instability arises. Its initial position is shown by the blue spot which quickly expands when the space charge tune shift increases (green and brown ovals). At $\Delta Q/Q_s = 3.69$, it reaches the primary zone of instability which is being situated at the left of the brown parabola at this instant. Barrier between the zones tears at higher ΔQ resulting in a single region of instability (red). Its right-hand boundary goes to the right, that is the TMCI threshold goes down, if the space charge tune shift continues to grow up.

For more explanation, real part of the same roots is plotted in Fig. 3 at $q < 0$. The most important curves are shown by bold lines, and the mode index is indicated near each of them. The TMCI threshold moves on the left in the beginning reaching $q_{\rm th}/Q_s \simeq -4$ at $\Delta Q/Q_s = 3.46$ by a merge of the modes {0,0}+{1,-1}

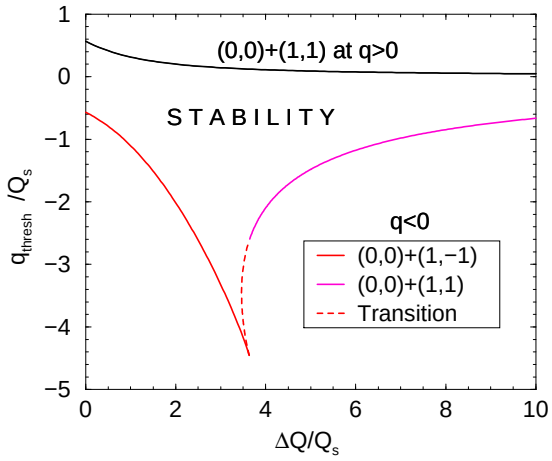

FIG. 4: Stability region of the boxcar bunch at positive (black) and negative (red+magenta) wakes.

(lower blue lines). However, the junction switches to the modes {0,0}+{1,1} at higher ΔQ resulting in the reverse motion of the threshold (higher red lines). The intermediate positions are shown by thin dashed line.

Total region of stability in $(\Delta Q - q)$ plane is shown in Fig. 4 with both positive and negative wakes taken into account. The complicated shape of the red curve is explained just by the additional instability region which appears at $\Delta Q/Q_s = 3.46$ and is represented in the picture by the dashed red line.

Eigentunes on boundary of this area are shown in Fig. 5. Generally, there are 3 real roots in the stability region but at least 2 of them coincides on the boundary. Therefore not more than 2 lines of each

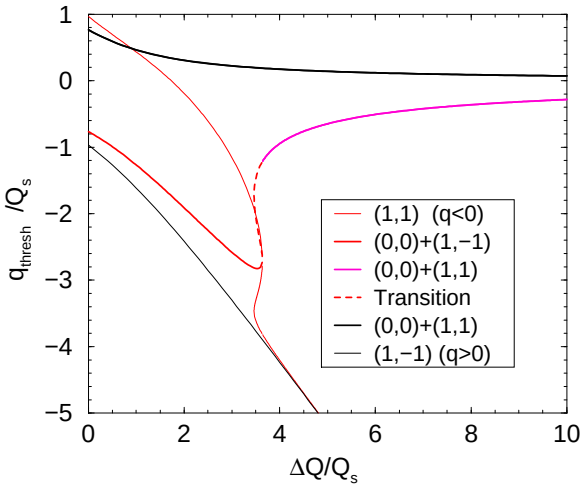

FIG. 5: The bunch eigentunes on boundaries of the stability region. With positive wake, the TMCI appears as a coalescence of the modes $\{0,0\}$ and $\{1,1\}$ (thick black line). With negative wake, the modes $\{0,0\}+\{1,-1\}$ coalesce at $\Delta Q/Q_s < 3.46$, and $\{0,0\}+\{1,1\}$ modes do it at $\Delta Q/Q_s > 3.69$. There is a transition region where all tunes about coincide.

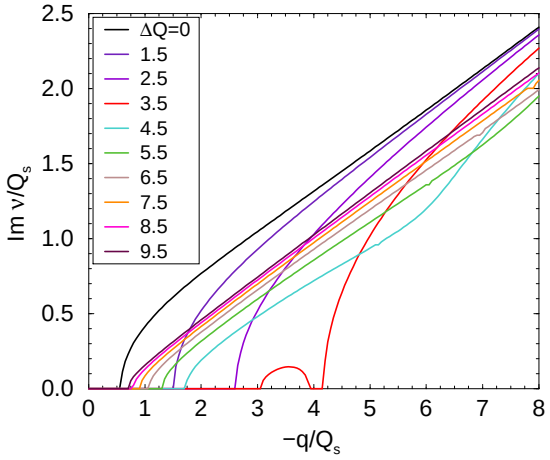

FIG. 6: Instability growth rate vs wake strength (three-mode model, negative wake).

color are visible in the picture. With negative wake, the modes $\{0,0\}+\{1,-1\}$ coalesce at $\Delta Q/Q_s < 3.46$, and $\{0,0\}+\{1,1\}$ modes do it at $\Delta Q/Q_s > 3.69$. There is a transition region where all tunes about coincide. The black curves for positive wake are very simple: the top line represents the coalesced modes $\{0,0\}+\{1,1\}$, and the bottom line is tune of the last mode $\{1,-1\}$.

The instability growth rate in this approximation is plotted in Fig. 6 being shown against the wake strength at different space charge tune shifts. The uprise of the additional instability region is seen here as well (red line).

V. HIGHER APPROXIMATIONS

Higher approximations should be considered to validate the three-mode model, to establish its applicability limit, and to go beyond it. The first step in this direction is investigation of the equation $T_2(\nu)=0$. According to Eq. (19)-(20), its expanded form is

$$\nu - q + \frac{q^2 W_1(\nu)}{9} + \frac{q^2(\nu-q)W_1(\nu)W_2(\nu)}{225} = 0 \quad (22)$$

where

$$W_1(\nu) = \frac{3(\nu+\Delta Q)}{\nu(\nu+\Delta Q) - Q_s^2}, \quad (23a)$$

$$W_2(\nu) = \frac{|S_{2,-2}|^2}{\nu-\nu_{2,-2}} + \frac{|S_{2,0}|^2}{\nu-\nu_{2,0}} + \frac{|S_{2,2}|^2}{\nu-\nu_{2,2}} \quad (23b)$$

Required parameters have to be obtained by solution of Eq. (11) with $n=2$ which procedure is described in the Appendix. With the notations $\nu_{n,m} = \hat{\nu}_{n,m}Q_s + \Delta Q$, the eigentunes appear as roots of the dispersion equation

$$\hat{\nu}_{2,m}(\hat{\nu}_{2,m}^2 - 4) = \frac{\Delta Q}{Q_s}(\hat{\nu}_{2,m}^2 - 1) \quad (24)$$

and the formula for corresponding normalizing coefficients is

$$|S_{2,m}|^2 = \frac{5(\hat{\nu}_{2,m}^2-1)^2}{\hat{\nu}_{2,m}^4 + \hat{\nu}_{2,m}^2 + 4} \quad (25)$$

Substitution of the functions $W_{1-2}(\theta)$ into Eq. (22) result in the equation

$$(\nu-q)\left(\nu - \frac{Q_s^2}{\nu+\Delta Q}\right) + \frac{q^2}{3} = -\frac{q^2(\nu-q)}{75}\left(\frac{|S_{2,-2}|^2}{\nu-\nu_{2,-2}} + \frac{|S_{2,0}|^2}{\nu-\nu_{2,0}} + \frac{|S_{2,+2}|^2}{\nu-\nu_{2,+2}}\right) \quad (26)$$

Its real roots can be found numerically. Number of the roots is 6 but only 5 different ones can appear in the boundary of the stability region. It is just the way to find the threshold value of the wake as well as corresponding eigentunes of the system with given ΔQ. The result is presented in Fig. 7 by red line.

Similar method can be used for analysis of higher approximations as well, thought the corresponding formulae are more cumbersome. Generally, it leads to the algebraic equation of power $(n_{\max}+1)(n_{\max}+2)/2$ where $n_{\max}$ is the power of the highest used Legendre polynomial.

Some results of the calculations are represented in Fig. 7-8 where q_{th}/Q_s is plotted against $\Delta Q/Q_s$ at $n_{\max} = 1-10$. It should be noted at once that the effect of positive wake almost does not depend on the power of

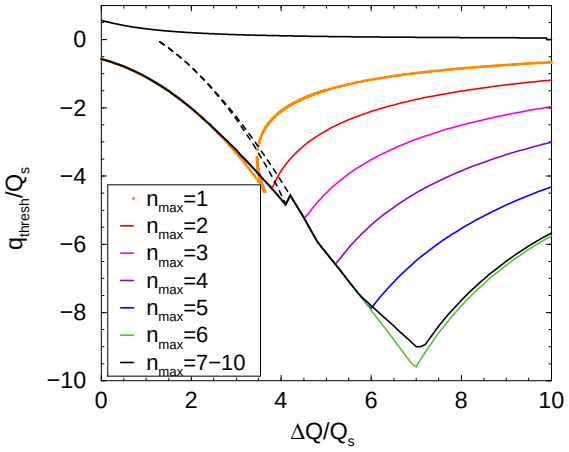

FIG. 7: Stability region of the boxcar bunch at different approximations. Index $n_{\max}$ means maximal power of polynomial in the expansion. The top black curve refers to positive wake with any $n_{\max}$, and others refer to negative wakes. The dashed lines mark a narrow strip of instability inside the wide stable area which appears at $n_{\max} \geq 3$.

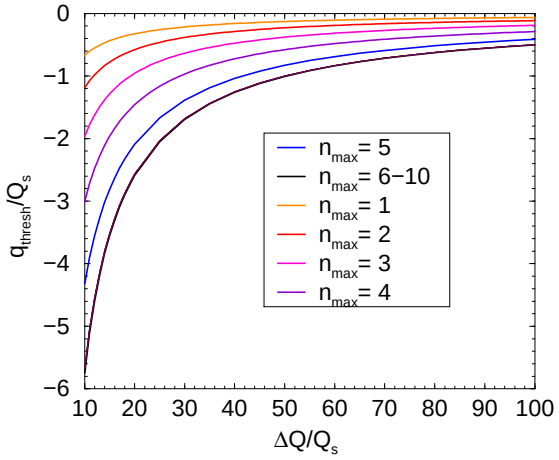

FIG. 8: Same as in Fig. 7 with higher ΔQ. The curves with $n_{\max} \geq 6$ are indistinguishable in this plot.

the polynomial, and can be reasonably described by the three-mode Eq. (21). Therefore only the case of negative wake is commented below.

The curves in Fig. 7-8 are well converging, so that any approximation $n_{\max} \geq 6$ can be safely used with any ΔQ. However, the lower order approximations could be sufficient if the tune shift is not so large. In particular, three-mode approximation ($n_{\max} = 1$) provides well accuracy at $\Delta Q/Q_s < 3.5$. The case $n_{\max} = 5$ (21 modes) is applicable at $\Delta Q/Q_s < 6$ but underestimates the TMCI threshold by ∼25% at larger value of the shift. It is necessary to pay an attention to the narrow strip of instability which becomes apparent at $n_{\max} \geq 3$ being marked by the dashed lines in Fig. 7. Its sense and cause will be explained two paragraphs below.

Important conclusions can be derived by analysis of the boundary spectrum that is the bunch tunes $\nu_{th}(\Delta Q)$ at the frontier of the TMCI zone. Very first example has been represented in Fig. 5 by analysis of three-mode approximation ($n_{\max} = 1$). It was shown that the sudden veer of the curve $\nu_{th}(\Delta Q)$ happens when the tune coupling switches from the modes $\{0,0\} + \{1,-1\}$ to $\{0,0\} + \{1,1\}$

The case $n_{\max} = 4$ is represented in Fig. 9. All 15 tunes of this approximation are shown in the graph, and the most important of them are accentuated by the bold lines and inscriptions. In the beginning, the TMCI occurs due to coupling of the modes $\{0,0\}$ and $\{1,-1\}$ which are shown by red lines. Then it passes through the $\{2,0\} + \{1,1\}$ coalescence (green lines) to the final combination $\{3,3\} + \{4,4\}$ (blue). Each step is followed by a veer of the threshold curve (dashed black line). Other short-time conjunctions or crossings of the spectral lines

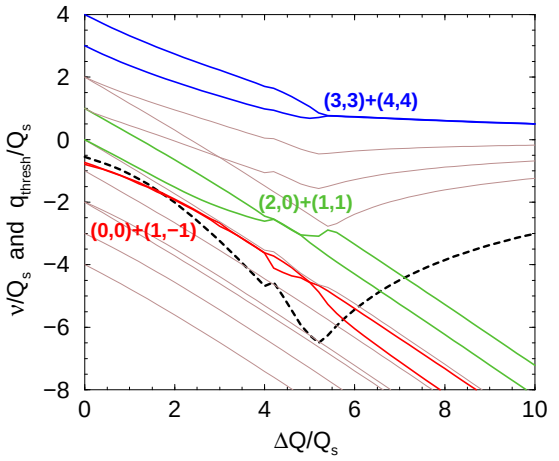

FIG. 9: The bunch spectrum in the TMCI frontier at $n_{\max} = 4$ (15-mode approximation). The most important modes are shown by solid bold lines and supplied with inscriptions. The TMCI threshold is represented by dashed black line.

are seen in the picture as well. They can be responsible for petty areas of instability one of which is marked in Fig. 7 by dashed lines. Perhaps, there are other similar zones but they are elusive because of small size.

Similar behavior of the spectrum is demonstrated in Fig. 10 where the case $n_{\max} = 7$ is considered. However, there is an important difference from previous example because the ultimate coupling of the modes $\{4,4\}+\{5,5\}$ happens inside the spectrum, and there are 2 tunes above the junction. It confirms that the saturation is achieved at $n_{\max} = 6$, and additional basis vectors no longer affect the mode coupling.

Summarizing this section, one can propose following

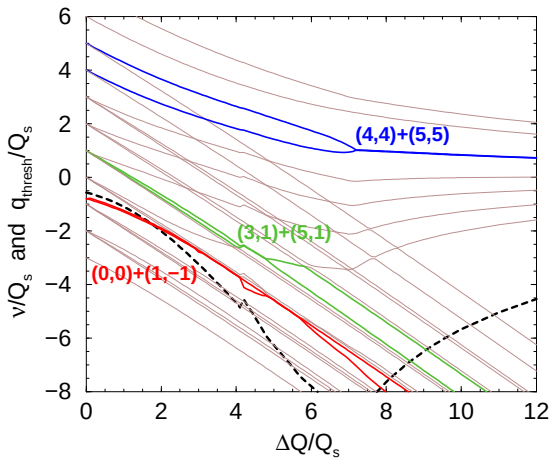

FIG. 10: The same as Fig. 9 at $n_{\max} = 7$ (35 modes).

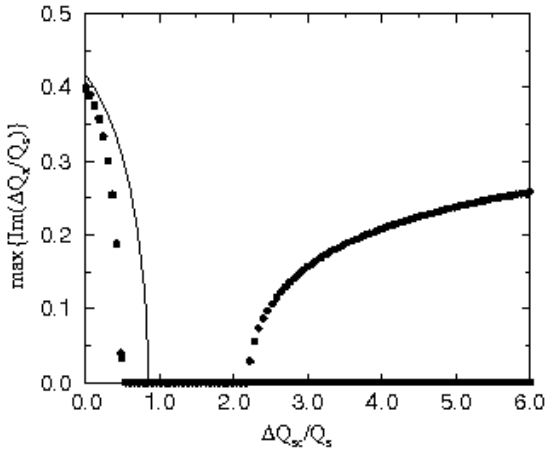

FIG. 1. Largest value of $\mathrm{Im}(\Delta Q_x/Q_s)$ as a function of $\Delta Q_{sc}/Q_s$ and m_{max} using matrix element (12). The value of W is twice the size needed to produce instability with $\Delta Q_{sc} = 0$: $m_{max} = 1$, solid line; $m_{max} = 5$, squares; $m_{max} = 10$, circles.

Copy of Fig. 1 [3]

approximate formulae for negative wake:

$$q_{th} \simeq \begin{cases} -\sqrt{(0.57Q_s)^2 + (1.3\Delta Q)^2} & \text{at} \quad \Delta Q/Q_s < 7 \\ -50Q_s^2/\Delta Q & \text{at} \quad \Delta Q/Q_s > 7 \end{cases} \tag{27}$$

The case of positive wake is much simpler: TMCI is caused by a coupling of the modes $\{0,0\}+\{1,1\}$ at any ΔQ, and three-mode approximation is sufficient for the calculation resulting in the threshold formula

$$q_{th} \simeq 0.57\left(\sqrt{Q_s^2 + \frac{\Delta Q^2}{4}} - \frac{\Delta Q}{2}\right) \tag{28}$$

Eq. (27)-(28) are the fits of Fig. 7-8 providing the accuracy not worse of 15% at any tune shift.

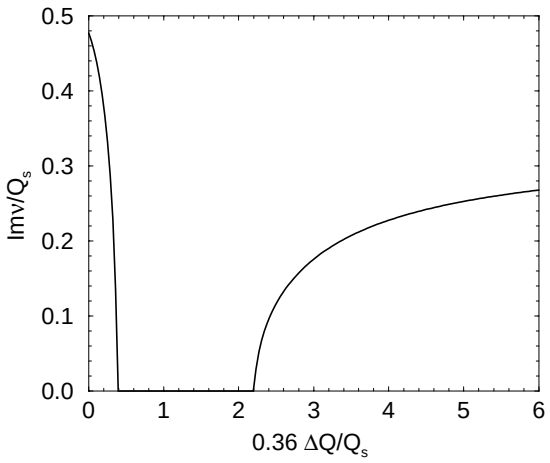

FIG. 11: TMCI growth rate against space charge tune shift by [3] (top) and by Eq. (21) (bottom), at fixed wake strength $q = -1.13$.

VI. DISCUSSION

Comparison of the results with published papers is the subject of this section.

Fig. 1 of Ref. [3] is reproduced in upper Fig. 11 of this paper. The TMCI growth rate is plotted in the graph against the tune shift at fixed wake strength which corresponds to $q = -1.13$ in my terms. The same function is plotted in lower Fig. 11 which is calculated by solution of Eq. (21). It would be possible to tell about amazing similarity of the pictures if not the difference of the horizontal scales. According to the upper graph, the space between two instability regions is $\Delta Q/Q_s = 1.4$ whereas it should be about 3 times more by the bottom plot. Another important thing is that the second region of instability appears only in the high-mode approximation $m_{\max} = 10$ in the upper picture. However, it would be situated far to the right ($\Delta Q/Q_s >\sim 45$) if corresponding high-order approximation is used for the lower graph. Therefore, one can declare only qualitative agreement with this result of the paper [3]. Another model of Ref. [3] is a hollow bunch in the square potential well. In contrast with previous, it predicts a monotonic growth of the TMCI threshold at increasing tune shift.

There is a better agreement with Ref. [6] where results of numerical simulations are represented. Shape of the threshold curve with negative wake is very similar to Fig. 7 at $\Delta Q/Q_s \leq 6$, and there is a rather good quantitative agreement. For example, both papers give $q_{th}/Q_s \simeq -6.5$ at $\Delta Q/Q_s = 5$. Thresholds of positive wakes are in a full consent as well.

The case $\Delta Q \to \infty$ is more complicated and requires a careful consideration. It follows from Fig. 7-8 and Eq. (27)-(28) that the TMCI threshold tends to 0 in this

limit. In contrast, it was argued in papers [4] and [5] that negative wake can't cause TMCI at all at such conditions ("vanished TMCI [4]"). It was noted in the Introduction that this statement is questionable because negative multipoles have been actually excluded from the consideration in mentioned papers. However, we can see now that this objection is certainly essential only at $\Delta Q/Q_s <\sim 7$ and maybe is not so important at higher ΔQ where the instability is caused just by coupling of positive multipoles (see Fig. 10).

It should be noted in this connection that central equations of the quoted papers could be solved for the boxcar bunch by the method which is developed in this paper. It would result in Eq. (17) with additional conditions:

$$\nu_{n,n} = \frac{Q_s^2 n(n+1)}{2\Delta Q} \tag{29a}$$

$$|S_{n,m}|^2 = (2n+1)\,\delta_{n,m}, \tag{29b}$$

which are simply the asymptotic values of these parameters at $\Delta Q \to \infty$. However, truncation of significant part of the spectrum produced by Eq. (29b) crucially changes the result. It is illustrated by Fig. 12 which is obtained by solution of Eq. (18) with assumptions (29) at different $n_{\max}$. The graph drastically differs from Fig. 8 though both of them are calculated by the same method but with/without the truncation. Despite the poor convergence of the curves in Fig. 12, trend to the threshold growth is evident. However, it is seen now that this conclusion is unreliable and should be rejected if tune shift exceeds synchrotron tune on one or two orders of value. It confirms the supposition which can be expressed first by Burov [4].

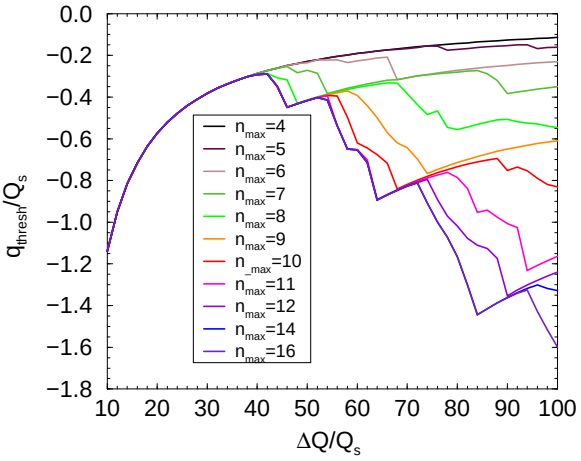

FIG. 12: TMCI threshold with the limiting parameters described by Eq. (29). Top black line: $n_{\max} = 2-4$, further $n_{\max} = 5-16$, $\Delta n = 1$.

VII. CONCLUSION

Being stable in themselves, eigenmodes of the boxcar bunch with space charge form convenient and effective basis for investigation of the bunch instability with space charge and wake field. Dispersion equation derived by this method is represented in the form of infinite continued fraction as well as in the form of recursive relation with arbitrary number of the basis vectors included.

It is shown that effect of the space charge on the instability essentially depends on the wake sign. TMCI threshold of positive wake goes down monotonously when the space charge tune shift increases as it is approximately described by Eq. (28). The negative wake threshold goes up in absolute value if $\Delta Q/Q_s < 7$, and goes down at higher $\Delta Q/Q_s$, Eq. (27). Such a complicated behavior occurs because the coalescence of different modes is responsible for the instability at different $\Delta Q/Q_s$. If the wake is negative, the multipoles $m = 0$ and $m = -1$ are coupled at lower ΔQ and $m = 6-7$ at higher one. The rearrangement comes with an abrupt dog-leg of the threshold curve. With positive wake, the multipoles $m = 0$ and $m = 1$ are responsible for the instability at any tune shift resulting in monotonous decrease of the threshold. Additional investigation of variable wakes looks to be important.

VIII. ACKNOWLEDGMENTS

FNAL is operated by Fermi Research Alliance, LLC under contract No. DE-AC02-07CH11395 with the United States Department of Energy.

IX. APPENDIX

Using the notation

$$\hat\nu_{n,m} = \frac{\nu_{n,m} + \Delta Q}{Q_s}, \quad \hat\Delta Q = \frac{\Delta Q}{Q_s}, \quad P_n(\theta) = \sum_{l=0}^{n} p_{nl}\theta^l \tag{A1}$$

one can write Eq. (11) in the form

$$\hat\nu_{n,m} Y_{n,m} + i\,\frac{\partial Y_{n,m}}{\partial\phi} = S_{n,m}\Delta\hat Q \sum_{l=0}^{n} p_{n,l}(A\cos\phi)^l \tag{A2}$$

Its solution is

$$Y_{n,m} = S_{n,m}\Delta\hat Q \sum_{k=-n}^{n} \frac{\exp ik\phi}{\hat\nu_{n,m} - k} \sum_{j=0}^{n} U_{n,k,j} A^{k+2j} \tag{A3}$$

where

$$U_{n,k,j} = \frac{p_{n,k+2j}}{2^{k+2j}} \binom{k+2j}{j} \times \begin{cases} 1 & \text{at} \quad k+j \ge 0 \\ 0 & \text{at} \quad k+j < 0 \end{cases} \tag{A4}$$

This function should satisfy normalization condition represented by Eq. (6) with $j \equiv \{n,m\}$ and distribution function (10a). The substitution results in the relation:

$$1 = \sum_{k=-n}^{n} \frac{S_{n,m}^2 \Delta\hat{Q}^2}{(\hat{\nu}_{n,m}-k)^2} \sum_{j_1=0}^{n}\sum_{j_2=0}^{n} U_{n,k,j_1} U_{n,k,j_2} \overline{A^{2(k+j_1+j_2)}} \tag{A5}$$

where $\overline{A^{2j}}$ is the amplitude power averaged over the distribution:

$$\overline{A^{2j}} = \int_0^1 \frac{A^{2j+1}\,dA}{\sqrt{1-A^2}} = \sum_{l=0}^{j} \binom{j}{l} \frac{(-1)^l}{2l+1} \tag{A6}$$

In principle, involved eigentunes $\nu_{n,m}$ could be obtained by substitution of Eq. (A3) into Eq. (3) with the functions Y and $\bar{Y}$ being taken from this Appendix. Because similar calculation has been actually accomplished in Ref. [8], we represent here only the resulting equation for the eigentunes:

Lower powers

$$\hat{\nu}_{0,0} = \Delta\hat{Q}, \qquad \hat{\nu}_{1,\pm1}^2 - 1 = \Delta\hat{Q}\hat{\nu}_{1,\pm1} \tag{A7}$$

Higher even powers

$$\hat{\nu}_{n,m}[\hat{\nu}_{n,m}^2 - 4]\ldots[\hat{\nu}_{n,m}^2 - n^2]$$

$$= \Delta\hat{Q}[\hat{\nu}_{n,m}^2 - 1]\ldots[\hat{\nu}_{n,m}^2 - (n-1)^2] \tag{A8}$$

Higher odd powers

$$[\hat{\nu}_{n,m}^2 - 1]\ldots[\hat{\nu}_{n,m}^2 - n^2]$$

$$= \Delta\hat{Q}\hat{\nu}_{n,m}[\hat{\nu}_{n,m}^2 - 4]\ldots[\hat{\nu}_{n,m}^2 - (n-1)^2] \tag{A9}$$

Some of the values $\nu_{n,m}/Q_s = \hat{\nu}_{n,m} - \Delta\hat{Q}$ are plotted in Fig. 1. Factors $S_{n,m}^2$ can be found from Eq. (A5) with the known eigentunes substituted. Some results are represented below:

$$S_{0,0}^2 = 1, \qquad S_{1,\pm1}^2 = \frac{3\hat{\nu}_{1,\pm1}^2}{\hat{\nu}_{1,\pm1}^2 + 1}\,, \tag{A10}$$

$$S_{3,m}^2 = \frac{5(\hat{\nu}_{2,m}-1)^2}{\hat{\nu}_{3,m}^4 + \hat{\nu}_{2,m}^2 + 4}\,, \tag{A11}$$

$$S_{3,m}^2 = \frac{7\hat{\nu}_{3,\pm1}^2(\hat{\nu}_{3,m}-4)^2}{\hat{\nu}_{3,m}^6 - 2\hat{\nu}_{3,m}^4 + 13\hat{\nu}_{2,m}^2 + 36}\,, \tag{A12}$$

etc.

[1] R. Kohaupt, in *Proceeding of the XI International Particle Accelerator Conference*, p.562, Geneva, Switzerland, (1980). DESY Rep. M-80/19 (1980).

[2] K. Y. Ng, "Physics of Intensity Dependent Beam Instabilities", Fermilab-FN-07-13 (2002).

[3] M. Blaskiewicz, Phys. Rev. ST Accel. Beams 1, 044201 (1998).

[4] A. Burov, Phys. Rev. ST Accel. Beams 12,044202 (2009).

[5] V. Balbekov, Phys. Rev. ST Accel. Beams 14, 094401 (2011).

[6] M. Blaskiewicz, in *Proceeding of International Particle Accelerator Conference (IPAC2012)*, May 20-25, New Orleans, USA, 2012, p. 3165.

[7] V. Balbekov, JINST 10 P10032 (2015) .

[8] F. Sacherer, CERN Rep. SI-BR-72-5 (1972).

[9] H. G. Hereward, CERN Rep. MPS-Int-DL-64-8 (1964).

[10] V. I. Balbekov, K. F. Gertsev, At.Energ.41 p.408 (1975). (DOI: 10.1007/BF01119511).